Materials Science and Engineering A 527 (2010) 3942–3948

Contents lists available at ScienceDirect

Materials Science and Engineering A

journal homepage: www.elsevier.com/locate/msea

Influence of grain size on the density of deformation twins in Cu–30%Zn alloy

Y. Li[a], Y.H. Zhao[a], W. Liu[a], C. Xu[b], Z. Horita[c], X.Z. Liao[d], Y.T. Zhu[e], T.G. Langdon[f,g,h], E.J. Lavernia[a,*]

[a] Department of Chemical Engineering & Materials Science, University of California, Davis, CA 95616, USA
[b] Ningbo Institute of Materials Technology and Engineering, Chinese Academy of Sciences, Ningbo, Zhejiang 315201, PR China
[c] Department of Materials Science and Engineering, Faculty Engineering, Kyushu University, Fukuoka 8128581, Japan
[d] School of Aerospace, Mechanical and Mechatronic Engineering, University of Sydney, NSW 2006, Australia
[e] Department of Materials Science and Engineering, North Carolina State University, NC 27695, USA
[f] Department of Aerospace & Mechanical Engineering, University of Southern California, Los Angeles, CA 90089-1453, USA
[g] Department of Materials Science, University of Southern California, Los Angeles, CA 90089-1453, USA
[h] Materials Research Group, School of Engineering Sciences, University of Southampton, Southampton SO17 1BJ, UK

ARTICLE INFO

Article history:
Received 2 February 2010
Received in revised form 24 February 2010
Accepted 25 February 2010

Keywords:
Nanostructured Cu–30%Zn alloy
Severe plastic deformation
Grain size
Deformation twin

ABSTRACT

Mechanical properties of nanostructured (NS) materials are significantly affected by both grain size and twin density, and the twin density has a close relationship with the grain size. Therefore, it is fundamentally important to understand the influence of grain size on the density of deformation twins in NS materials. In this study, we selected Cu–30%Zn alloy as a model material to study this phenomenon, because it has low stacking fault energy of 7 mJ m^{-2} and twinning is its dominant deformation mechanism. High-pressure torsion (HPT), equal channel pressing (ECAP) and ECAP followed by rolling were used to achieve a wide range of grain size from about 3 μm to 70 nm. It is found that, with decreasing grain size, the average distance between deformation twins decreases gradually from 177 nm to 24 nm, while the density of deformation twins (the length of twin boundary in unit area) exhibit a maximum value at ECAP + 95% rolling sample with average grain size of 110 nm. Careful statistics analysis reveals two optimum grain size ranges 60–80 nm and 40–50 nm for maximum twin density values for ECAP + 95% rolling and HPT Cu–30%Zn samples, respectively. The underlying mechanisms governing the influence of grain size on twinning is discussed.

1. Introduction

Twinning in nanostructured (NS) metals and alloys has attracted extensive interest because both pre-existed twin boundaries (TBs) and deformation twinning have been demonstrated to improve the ductility of bulk NS materials [1–4]. In addition, deformation twinning has also been reported as one of the important deformation mechanisms of bulk NS materials [5–7]. The high-density pre-existing TBs improve the poor ductility of bulk NS materials by increasing both strain hardening and strain-rate sensitivity [8–9]. The strain hardening increase has resulted from the interaction between the TBs and dislocations as the TBs gradually lose coherency during plastic deformation [10]. In addition to enhancing strain hardening rate, the deformation twinning itself also facilitates some plastic strain [3–4].

From the above discussion, it is clearly important to engineer high density of TBs into NS grains for good mechanical properties. A careful inspection of the related literature indicates that the propensity of deformation twinning in metals and alloys is affected by the following factors: the stacking faults energy (SFE), deformation strain rate and temperature, and grain size [10–17]. It is widely known that metals and alloys with a low SFE readily deform via twinning [10]. High strain rates and low temperatures also facilitate twinning in the face-centered cubic (fcc) metals such as Cu and Ni, which do not typically deform by twinning under normal deformation conditions due to their relatively high SFE values [11,12]. Grain size is an essential factor that affects the formation of deformation twins in metals and alloys. It has been extensively reported in the literature that larger grain sizes are more favorable to twin nucleation for conventional coarse-grained (CG) materials [6,13,15,18].

The influence of grain dimensions on twinning may be rationalized as follows. At room temperature, both the critical stresses σ for dislocation slip and twinning follow a Hall–Petch-type (H–P) behavior, $\sigma = \sigma_0 + kd^{\alpha}$, where d is grain size, σ_0 and k are grain size independent constants and α is an exponent typically equal to 0.5. For many CG metals and alloys, the H–P slope for deformation-twinning-mediated plasticity (k_{DT}) is much larger (up to 10 times) than that for dislocation slip (k_{DS}) [19–20]. This makes dislocation slip the preferred plastic deformation mode when d is smaller

* Corresponding author.
E-mail address: lavernia@ucdavis.edu (E.J. Lavernia).

0921-5093/$ – see front matter © 2010 Elsevier B.V. All rights reserved.
doi:10.1016/j.msea.2010.02.076

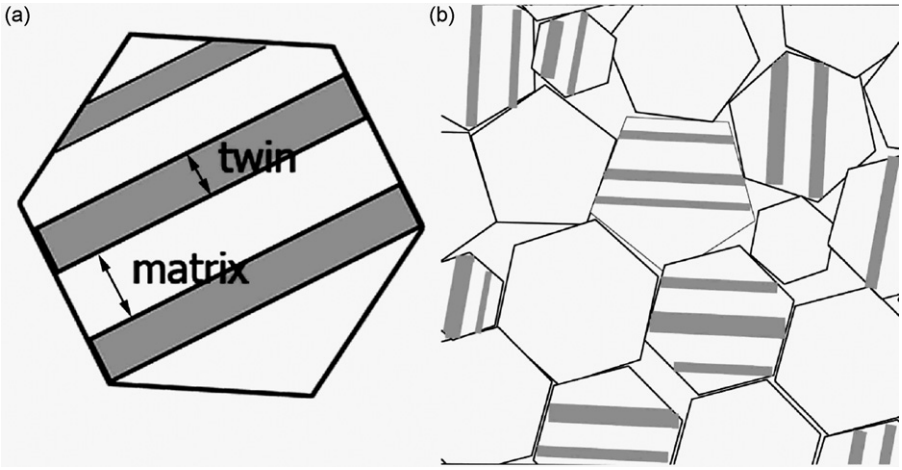

Fig. 1. (a) Schematical representation of the twin ribbon and matrix in a grain. (b) Schematic of counting method of twin density.

than a certain value [21]. However, when the grain size is further refined down to nanometer regions (for example smaller than 50 nm), deformation twinning has been frequently observed even in materials with medium to high stacking fault energies such as copper and nickel, and therefore was treated as one of the major plastic deformation mechanisms of NS materials [22–25]. Systematic high-resolution transmission electron microscopy revealed that the deformation twinning of nanostructured materials was formed by Shockley partial dislocation emissions from grain boundaries [26,27]. More recent study indicates that further decreasing the grain size of nanostructured materials impedes twinning (i.e. inverse grain size effect), which was explained using generalized planar fault energies and grain-size effect on partial emissions [16].

In this work, to systematically study the grain size effect on the characteristics of deformation twinning, we selected Cu–30%Zn (wt% except as noted) alloy as our model material, because it readily forms twins due to its low SFE (7 mJ m^{-2}) [28]. Three processing methods, equal channel pressing (ECAP), ECAP followed by rolling, and high-pressure torsion (HPT), were used to produce grains wide ranges of sizes. The grain size and twin characteristics, including widths of twin and matrix plates, and twin density (entire length of TB in unit area) were systematically studied using transmission electron microscopy (TEM).

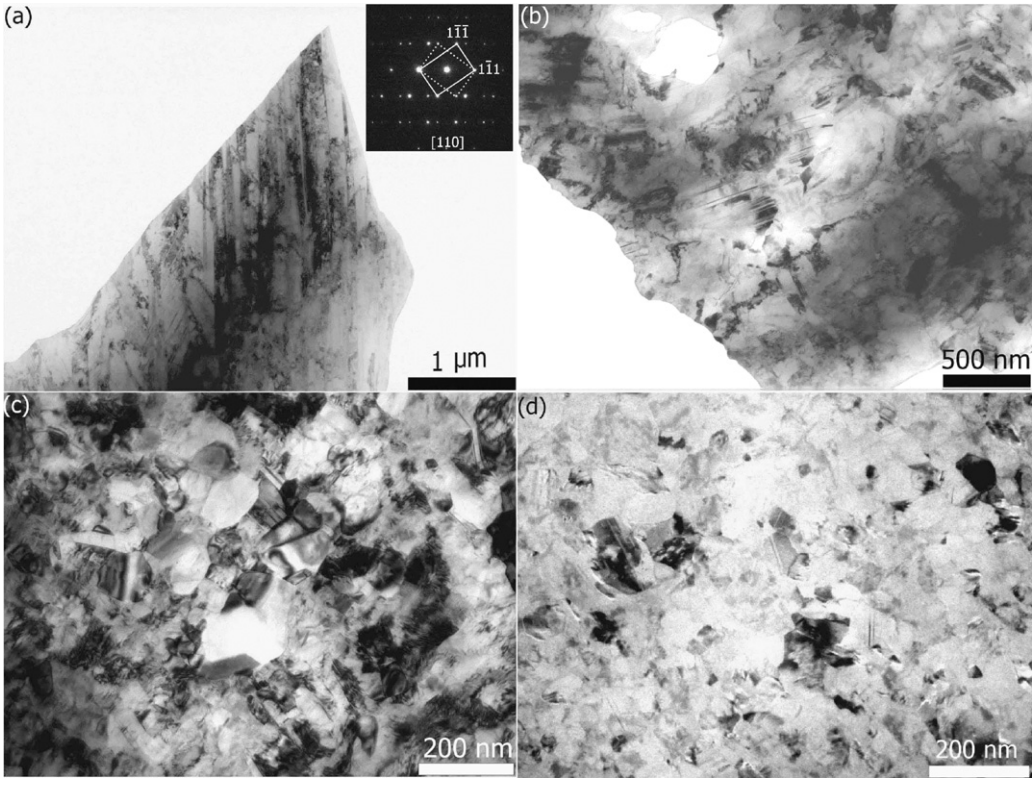

Fig. 2. TEM images showing the typical morphology and twin characteristics of the (a) ECAP, (b) ECAP + 75% rolling, (c) ECAP + 95% rolling, and (d) HPT Cu–30%Zn samples. The inset in (a) is the corresponding selected area electron diffraction (SAED) pattern verifying the existence of twins.

Table 1
Lists of average grain size, twin width, matrix width and twin density of the ECAP, ECAP + 75% rolling and ECAP + 95% rolling, and HPT samples.

Samples	Grain size (nm)	Twin width (nm)	Matrix width (nm)	Twin density (10^6 m^{-1})
ECAP	3000	90	177	3.5
ECAP + 75% rolling	355	17	32	6.9
ECAP + 95% rolling	110	12	24	11.2
HPT	70	11	31	8.3

2. Experimental

Commercial pure Cu–30%Zn alloy was received in the form of rods with a diameter of 10 mm. Disks with a diameter of 10 mm and a thickness of 0.8 mm, prepared from the as-received rods, were placed between two anvils and HPT processed at room temperature under an imposed pressure of 6 GPa for five rotations with a rotation speed of 1 rpm; details can be found in [29]. In the case of ECAP, the as-received rods were annealed at 600 °C for 1 h, and then ECAP-processed at 220° for 3 passes by Bc route [30] using a die with a channel angle of 90° to give a strain of about 1 on each pass [31]. The as-processed rods were then sectioned into plates and cold rolled at room temperature into thin plates with thickness reductions of 75% and 95% (designated samples ECAP + 75% rolling and ECAP + 95% rolling thereinafter), respectively. The rolling direction is parallel to the longitudinal axis of the rod.

TEM specimens were prepared by mechanically grinding the bulk materials to a thickness <30 μm, then dimpling from both sides to a thickness of approximately 10 μm. Further thinning to a thickness of electron transparency was carried out using a Gatan PIPS 691 ion milling system at a voltage of 4 kV. Morphology images and selected-area electron diffraction (SAED) patterns of the samples were taken on a Philips CM12 transmission electron microscope at a voltage of 100 kV.

The widths of the twin and matrix are two parameters that can be used to characterize twin structures in a metal, as noted by Xiao et al. [32]. In their work, the widths of twin and matrix were measured from dark field images attained by selecting a diffraction spot that originated from the twin structure using an objective aperture. However, this method could not be applied to the present ECAP+ rolling and HPT samples because their grain sizes are too small to obtain an SAED pattern for an individual grain; in fact the diffraction spots corresponding to the twin and matrix were not quite clear, either. In the present study, we define the width of the matrix is larger than the width of the twin, as shown schematically in Fig. 1a. We also define the twin density as the TB length in unit area. As shown in Fig. 1b, one twin ribbon will get two times length counted because it has two TBs. We calculated the overall length of the TBs from more than 20 TEM images with observation field of several μms, and then divided the length by the overall TEM image area. Note that different twin density values for the same twin structure may be obtained when the twin is observed under TEM from different orientations. However, statistically, the measured twin density can still reveal the trend of twin density evolution with decreasing grain size.

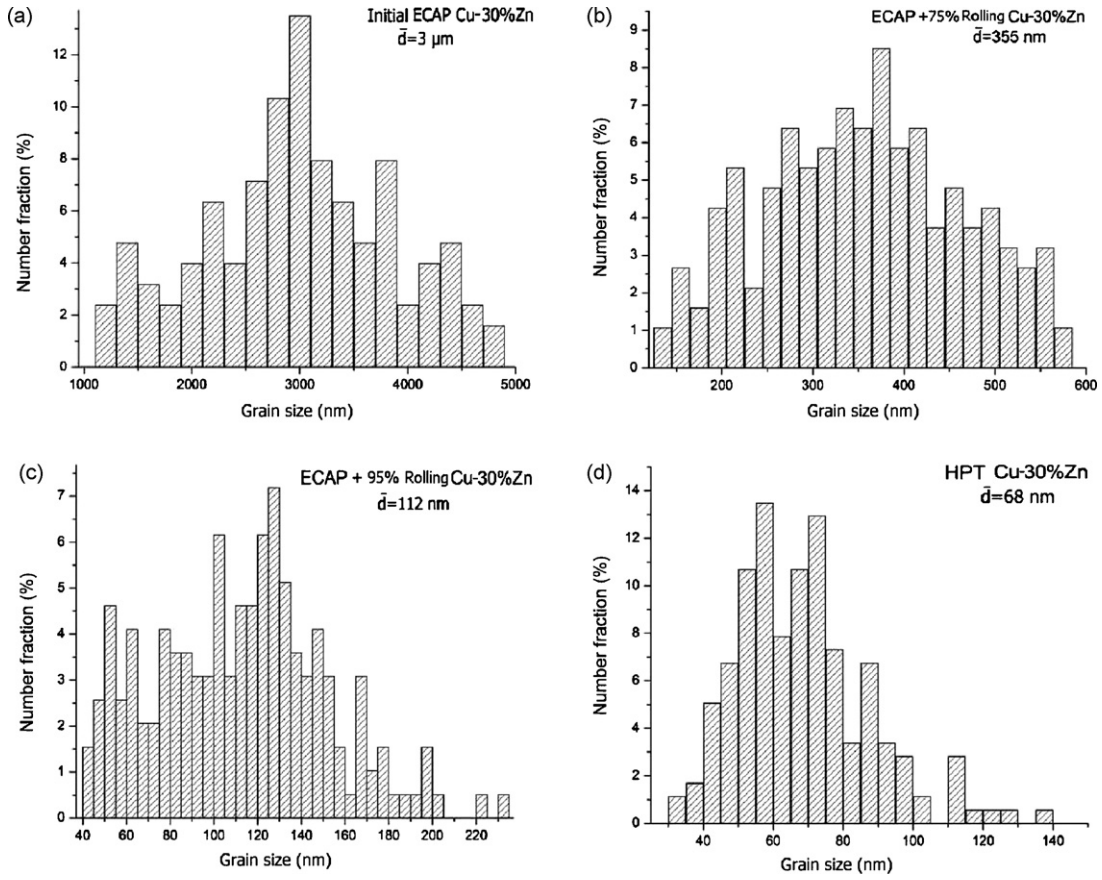

Fig. 3. Grain size histogram of the (a) ECAP, (b) ECAP + 75% rolling, (c) ECAP + 95% rolling and (d) HPT Cu–30%Zn samples.

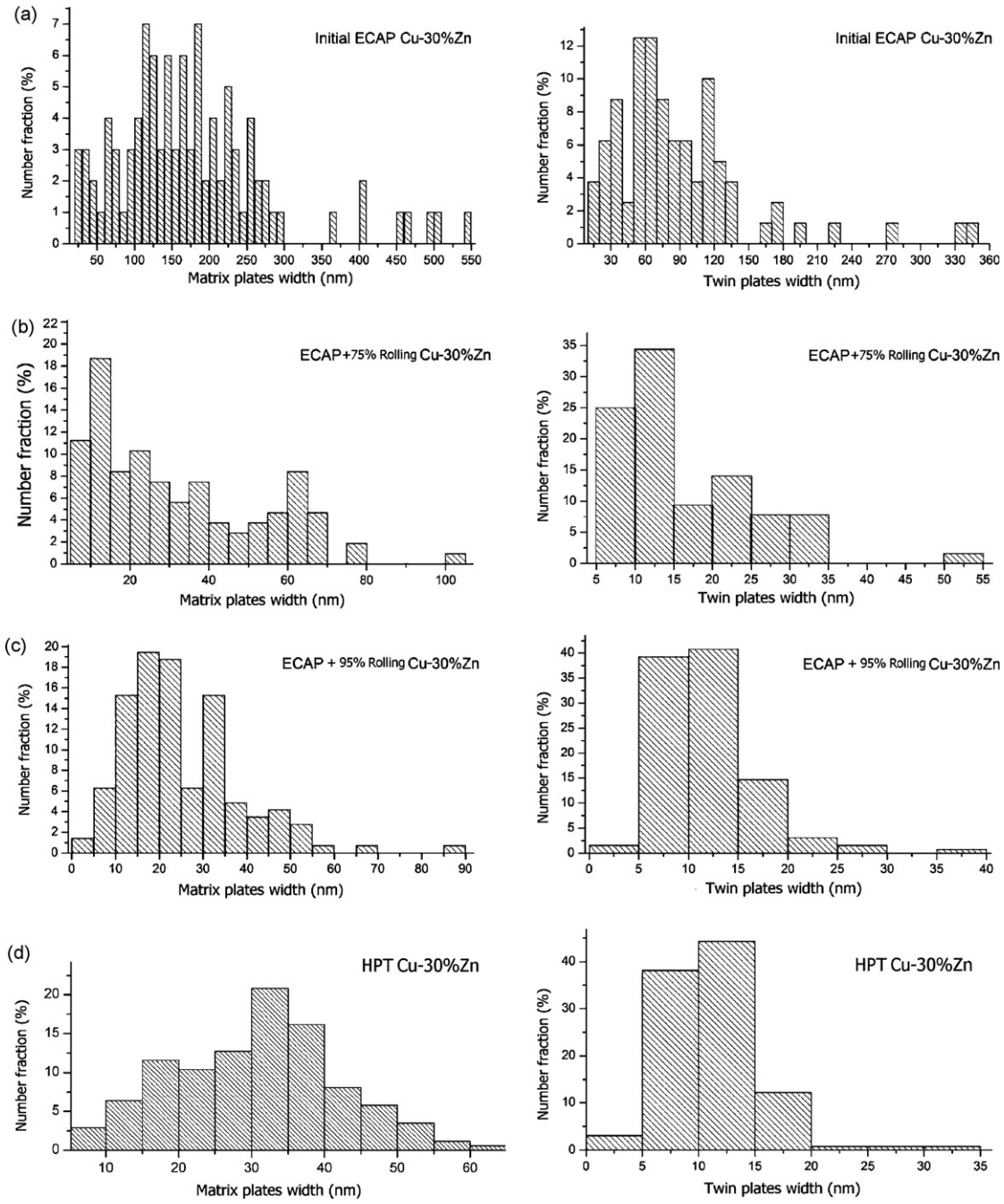

Fig. 4. Matrix and twin plate width histogram of (a) ECAP, (b) ECAP + 75% rolling, (c) ECAP + 95% rolling, and (d) HPT Cu–30%Zn samples.

3. Results

The TEM images shown in Fig. 2 illustrate the typical microstructures including grain size and twin characteristics of the samples: (a) ECAP, (b) ECAP + 75% rolling, (c) ECAP + 95% rolling, and (d) HPT. It is readily seen from the TEM images that the twin morphology in the ECAP sample is lamellar, with a length about 3 μm. The inserted selected area electron diffraction (SAED) pattern in Fig. 2a verified the existence of the twin. Rolling process gradually refined the grain size and broke the long twin ribbons (as shown in Fig. 2b and c). It is evident that the twin frequency appeared in the ECAP + 95% rolling sample is larger than that in the ECAP + 75% rolling sample due to larger plastic strain. Fig. 2d reveals a TEM image of the HPT samples, which the smallest grain size among the four samples has studied herein. The twin frequency is also very high: almost every grain contains one or multiple twins. Noteworthy is the fact that a significant proportion of the grains in the HPT sample contain a single twin.

To provide quantitative insight into the influence of process route on grain size and twin formation, we performed careful statistical analyses on the TEM images, and the results are summarized in Table 1 and Figs. 3–7. We counted about 100 grains for the ECAP sample and more than 200 grains for the other three samples to obtain grain size distributions, as shown in Fig. 3. The average grain size D is 3 μm, 355 nm, 110 nm and 70 nm for the ECAP, ECAP + 75% rolling, ECAP + 95% rolling and HPT samples, respectively.

Fig. 4a–d shows the histograms corresponding to the widths of the twin and matrix for the four samples, from which the average values can be determined and listed in Table 1 as well as shown in Fig. 5. There are two trends worth noting. First, the width of

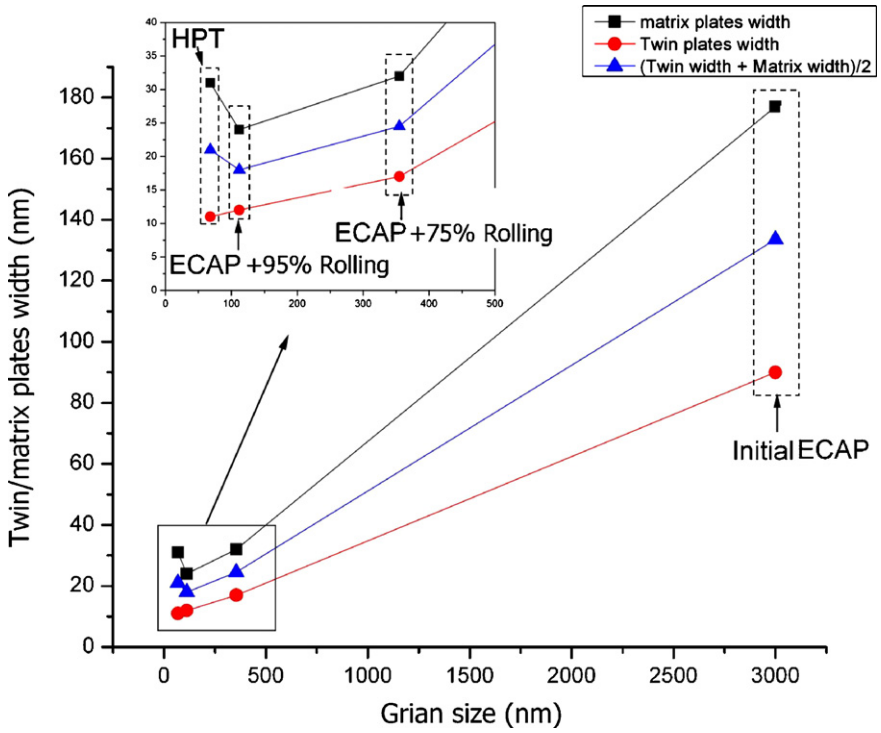

Fig. 5. Twin plate and matrix widths as well as their average values versus grain size (3 μm of sample initial ECAP, 355 nm of sample ECAP + 75% rolling, 110 nm of sample ECAP + 95% rolling, and 70 nm of sample HPT). The inset is a partially magnified image from the area that is indicated by arrow.

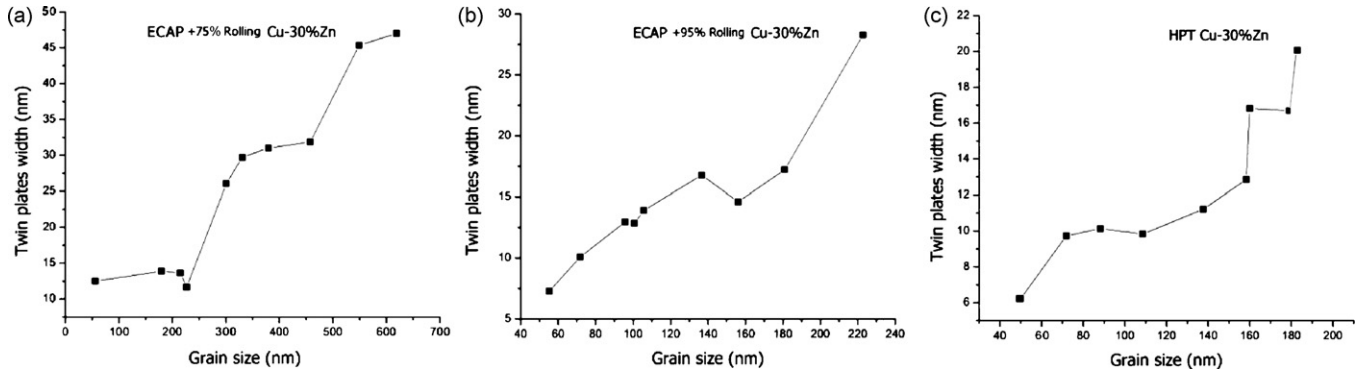

Fig. 6. The twin and matrix plate width fluctuation curve with different grain size in the same sample (received from same process method) for (a) ECAP + 75% rolling, (b) ECAP + 95% rolling, and (c) HPT Cu–30%Zn samples.

the matrix is almost twice as large as that of the twin for all four materials. Second, the average widths of the twin/matrix decreased from 90 nm/177 nm to 12 nm/24 nm when the grain size decreased from 3 μm to 110 nm. The average width saturated when the grain size further reduced to about 70 nm. To further verify the above dependence of twin width on grain size, we measured the twin widths in ten grains with different sizes from a single TEM specimen for the ECAP and ECAP + rolling samples, and the results are shown in Fig. 6. One can see that the twin width decreases as the grain size decreases in the same sample.

Fig. 7 shows the influence of grain size on twin density. One can see that with decreasing grain size, the twin density increases from $3.5 \times 10^6\ m^{-1}$ (3 μm) to $11.2 \times 10^6\ m^{-1}$ (110 nm), and drops down to $8.3 \times 10^6\ m^{-1}$ at a grain size of about 70 nm. This result indicates that rolling process gradually increases the twin density. However, the HPT sample has a lower twin density in comparison with the ECAP + 95% rolling sample but is higher than ECAP + 75% rolling sample. The ECAP sample exhibited the lowest twin density due to large twin width. Further rolling introduced more deforma-

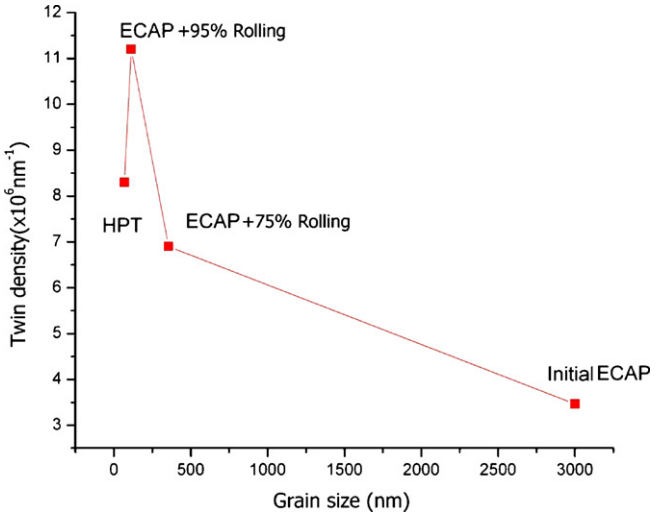

Fig. 7. The twin density against the average grain size for the four different samples.

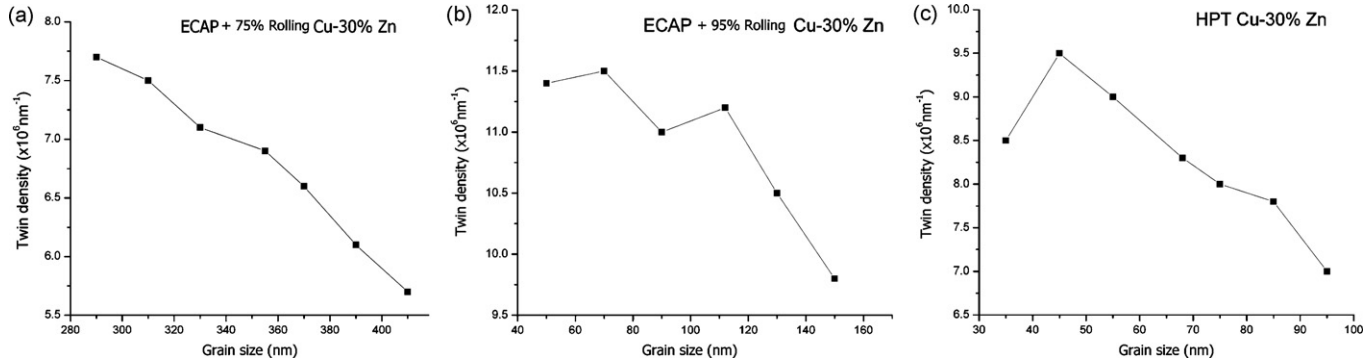

Fig. 8. The variations of twin density versus grain size for (a) ECAP + 75% rolling, (b) ECAP + 95% rolling, and (c) HPT Cu–30%Zn samples.

tion twins and therefore increased the twin density. Since many grains in HPT sample only have one or two twin plates, the amount of twin in one grain is smaller than that in the ECAP + 95% rolling samples. Therefore, the twin density in the HPT sample is lower than that in the ECAP + 95% rolling sample.

To further verify the maximum value of twin density, we measured the twin density in the grains with different sizes in a single TEM specimen for the ECAP + 75% rolling, ECAP + 95% rolling, and HPT samples. We checked more than 30 grains for each grain size range, such as from 60 nm to 80 nm for the ECAP + 95% rolling sample. A mean value was used to represent the grain size range in the statistical curves, for example, 70 nm was used to represent a grain size range of 60–80 nm. As shown in Fig. 8a, the twin density decreases with increasing grain size for the ECAP + 75% rolling sample. From Fig. 8b and c, we can see the twin density has a maximum value at 60–80 nm and 40–50 nm for ECAP + 95% rolling and HPT samples. These results indicate that the maximum twin density exists in a sample with grains in a certain size range, and it is independent of process conditions.

4. Discussion

As discussed in the introduction, when the grain size is refined to nanometer region (ultrafine grain region for Cu–30%Zn alloy), the twinning mechanisms operating in CG materials (e.g., the pole mechanism [33]) will be replaced by twinning via partial dislocation emission. In our previous study, we have verified that for Cu–10 wt.%Zn alloy with a stacking fault energy of 22 mJ m^{-2} [28], the critical grain size for partial emission can be larger than 120 nm [34]. As reported recently, partial dislocation emission from grain boundaries could also become a deformation mechanism in fcc metal with grain size range 100–500 nm during SPD [35]. So in our case, twinning by partial dislocation emission is also expected to occur in the ultrafine grained ECAP + 75% rolling Cu–30%Zn sample with a much larger average grain size because (1) Cu–30%Zn alloy has a much lower SFE (7 mJ m^{-2}) than Cu–10%Zn alloy, and (2) lowering SFE can increase the critical grain size for partial emission from grain boundaries. The newly formed twinning via partial emission by cold rolling further decreases the twin and matrix widths resulting in a decreasing twin width and increased twin density versus decreasing grain size.

Our results also indicate that there exists an optimum grain size for obtaining the highest twin density. That is, the twin density decreases again when the grain is refined beyond a critical size. The decreased twin density might be caused by the following reasons. First, it has been revealed that twin boundaries could be gradually transformed into normal high-angle grain boundaries by accumulation of dislocations at the TBs [36]. Second, de-twinning phenomena has been observed by in situ high-resolution transmission electron microscopy and molecular dynamic simulation in Cu films [37]. Third, the reported inverse grain size effect on twinning makes it more difficult to form twins in grains smaller than a critical size [16]. Higher stress is required to emit partials in smaller grains [38]. This means below a certain critical grain size, the critical stress required for emitting a twinning partial may become higher than the applied resolved shear stress, which makes the twinning more difficult. In addition, grain boundary sliding or grain rotation may become activated when the grain size become smaller, which releases the applied stress [7,39–41]. As discussed in the introduction part, the pre-existing twins not only enhanced the strength, but also stabilized the premature localized necking by increasing strain hardening rate and strain-rate sensitivity of bulk nanostructured materials. Therefore, our results on the optimum grain size for obtaining the highest twin density will provide guidance for designing nanostructured materials with both high strength and good ductility, that is, optimize strength and ductility by tailoring the optimum grain size with the highest twin density [42].

5. Conclusions

We have used different SPD methods to prepare bulk Cu–30%Zn alloys with an average grain size ranging from 70 nm to 3 μm. By TEM and statistical analysis, we found that:

1. The twin and matrix widths decrease with decreasing grain size.
2. The twin density increases with decreasing grain size and reaches a maximum value at a critical grain size. The optimum grain size for highest twin density is largely independent of processing conditions.
3. Below the critical grain size, twin density decreases when the grain size decreases further. This could be caused by the conversion of the twin boundary into grain boundary, detwinning process and the inverse size effect on deformation twinning.

Acknowledgement

The authors would like to acknowledge financial supports from the Office of Naval Research (Grant number N00014-08-1-0405).

References

[1] L. Lu, Y.F. Shen, X.H. Chen, L.H. Qian, K. Lu, Science 304 (2004) 422–426.
[2] Y.H. Zhao, J.E. Bingert, X.Z. Liao, B.Z. Cui, K. Han, A.V. Sergueeva, A.K. Mukherjee, R.Z. Valiev, T.G. Langdon, Y.T.T. Zhu, Adv. Mater. 18 (2006) 2949–2953.
[3] Y.H. Zhao, Y.T. Zhu, X.Z. Liao, Z. Horita, T.G. Langdon, Appl. Phys. Lett. 89 (2006) 121906.
[4] P.L. Sun, Y.H. Zhao, J.C. Cooley, M.E. Kassner, Z. Horita, T.G. Langdon, E.J. Lavernia, Y.T. Zhu, Mater. Sci. Eng. A 525 (2009) 83–86.
[5] V. Yamakov, D. Wolf, S.R. Phillpot, A.K. Mukherjee, H. Gleiter, Nat. Mater. 3 (2004) 43–47.
[6] M.W. Chen, E. Ma, K.J. Hemker, H.W. Sheng, Y.M. Wang, X.M. Cheng, Science 300 (2003) 1275–1277.

[7] X.Z. Liao, F. Zhou, E.J. Lavernia, S.G. Srinivasan, M.I. Baskes, D.W. He, Y.T. Zhu, Appl. Phys. Lett. 83 (2003) 632–634.
[8] L. Lu, R. Schwaiger, Z.W. Shan, M. Dao, K. Lu, S. Suresh, Acta Mater. 53 (2005) 2169–2179.
[9] T. Zhu, J. Li, A. Samanta, H.G. Kim, S. Suresh, Proc. Natl. Acad. Sci. U.S.A. 104 (2007) 3031–3036.
[10] J.A. Venables, Philos. Mag. 6 (1961) 379–396.
[11] T.H. Blewitt, R.R. Coltman, J.K. Redman, J. Appl. Phys. 28 (1957) 651–660.
[12] Y.S. Li, N.R. Tao, K. Lu, Acta Mater. 56 (2008) 230–241.
[13] K.P.D. Lagerlof, J. Castaing, P. Pirouz, A.H. Heuer, Philos. Mag. A 82 (2002) 2841–2854.
[14] M.R. Barnett, Scr. Mater. 59 (2008) 696–698.
[15] J.P. Hirth, J. Lothe, Theory of Dislocations, Krieger Publishing, Malabar,UK, 1992.
[16] X.L. Wu, Y.T. Zhu, Phys. Rev. Lett. 101 (2008) 025503.
[17] T. Saha, I. Dasgupta, A. Mookerjee, J. Phys.-Condes. Matter 8 (1996) 1979–1996.
[18] M.A. Meyers, U.R. Andrade, A.H. Chokshi, Metall. Mater. Trans. A 26 (1995) 2881–2893.
[19] M.A. Meyers, O. Vohringer, V.A. Lubarda, Acta Mater. 49 (2001) 4025–4039.
[20] E. El-Danaf, S.R. Kalidindi, R.D. Doherty, Metall. Mater. Trans. A 30 (1999) 1223–1233.
[21] Z.W. Shan, E.A. Stach, J.M.K. Wiezorek, J.A. Knapp, D.M. Follstaedt, S.X. Mao, Science 305 (2004) 654–657.
[22] X.Z. Liao, Y.H. Zhao, Y.T. Zhu, R.Z. Valiev, D.V. Gunderov, J. Appl. Phys. 96 (2004) 636–640.
[23] X.Z. Liao, Y.H. Zhao, S.G. Srinivasan, Y.T. Zhu, R.Z. Valiev, D.V. Gunderov, Appl. Phys. Lett. 84 (2004) 592–594.
[24] X.L. Wu, Y.T. Zhu, Appl. Phys. Lett. 89 (2006) 221911.
[25] X.L. Wu, E. Ma, Appl. Phys. Lett. 88 (2006) 121905.
[26] V. Yamakov, D. Wolf, S.R. Phillpot, A.K. Mukherjee, H. Gleiter, Nat. Mater. 1 (2002) 45–48.
[27] H. Van Swygenhoven, Science 296 (2002) 66–67.
[28] C.B. Carter, I.L.F. Ray, Philos. Mag. 35 (1977) 189–200.
[29] Y.H. Zhao, X.Z. Liao, Y.T. Zhu, Z. Horita, T.G. Langdon, Mater. Sci. Eng. A 410 (2005) 188–193.
[30] M. Furukawa, Y. Iwahashi, Z. Horita, M. Nemoto, T.G. Langdon, Mater. Sci. Eng. A 257 (1998) 328–332.
[31] Y. Iwahashi, J.T. Wang, Z. Horita, M. Nemoto, T.G. Langdon, Scr. Mater. 35 (1996) 143–146.
[32] G.H. Xiao, N.R. Tao, K. Lu, Scr. Mater. 59 (2008) 975–978.
[33] N. Thompson, D.J. Millard, Philos. Mag. 43 (1952) 422–440.
[34] Z.W. Wang, Y.B. Wang, X.Z. Liao, Y.H. Zhao, E.J. Lavernia, Y.T. Zhu, Z. Horita, T.G. Langdon, Scr. Mater. 60 (2009) 52–55.
[35] M.P. Liu, H.J. Roven, M. Murashkin, R.Z. Valiev, Mater. Sci. Eng. A 503 (2009) 122–125.
[36] Y.B. Wang, X.Z. Liao, Y.H. Zhao, E.J. Lavernia, S.P. Ringer, Z. Horita, T.G. Langdon, Y.T. Zhu, Mater. Sci. Eng. A, in review.
[37] J. Wang, N. Li, O. Anderoglu, X. Zhang, A. Misra, J.Y. Huang, J.P. Hirth, Acta Mater. 58 (2010) 2262–2270.
[38] Y.T. Zhu, X.Z. Liao, S.G. Srinivasan, Y.H. Zhao, M.I. Baskes, F. Zhou, E.J. Lavernia, Appl. Phys. Lett. 85 (2004) 5049–5051.
[39] H. Van Swygenhoven, P.A. Derlet, Phys. Rev. B 64 (2001) 224105.
[40] J. Schiotz, F.D. Di Tolla, K.W. Jacobsen, Nature 391 (1998) 561–563.
[41] S. Cheng, Y.H. Zhao, Y.Z. Guo, Y. Li, Q.M. Wei, X.L. Wang, Y. Ren, P.K. Liaw, H. Choo, E.J. Lavernia, Adv. Mater. 21 (2009) 5001–5004.
[42] Y.H. Zhao, X.Z. Liao, Z. Horita, T.G. Langdon, Y.T. Zhu, Mater. Sci. Eng. A 493 (2008) 123–129.